

Functional variants in *TNFAIP8* associated with cervical cancer susceptibility and clinical outcomes

Ting-Yan Shi^{1,2}, Xi Cheng^{2,3}, Ke-Da Yu^{2,4},
Meng-Hong Sun^{2,5}, Zhi-Ming Shao^{2,4}, Meng-Yun Wang^{1,2},
Mei-Ling Zhu^{1,2}, Jing He^{1,2}, Qiao-Xin Li^{1,2},
Xiao-Jun Chen^{2,3}, Xiao-Yan Zhou^{2,5}, Xiaohua Wu^{2,3,*}
and Qingyi Wei^{1,6}

¹Cancer Institute, Fudan University Shanghai Cancer Center, Shanghai 200032, China; ²Department of Oncology, Shanghai Medical College, Fudan University, Shanghai 200032, China; ³Department of Gynecologic Oncology; ⁴Department of Breast Surgery and ⁵Department of Pathology, Fudan University Shanghai Cancer Center, Shanghai 200032, China; and ⁶Department of Epidemiology, The University of Texas MD Anderson Cancer Center, Houston, TX 77030, USA

*To whom correspondence should be addressed. Department of Gynecologic Oncology, Fudan University Shanghai Cancer Center, 270 Dong An Road, Shanghai 200032, China. Tel: +86-21-64175590 ext.1006; Fax: +86-21-64220677;

Email: docwuxh@hotmail.com

Correspondence may also be addressed to Qingyi Wei, Cancer Institute, Fudan University Shanghai Cancer Center, Shanghai 200032, China. Tel: +86-21-64175590 ext. 5315; Fax: +86-21-64172585;

Email: weiqingyi@yahoo.com

Tumor necrosis factor- α -induced protein 8 (TNFAIP8) is an antiapoptotic and pro-oncogenic signaling molecule involved in the process of immunity, carcinogenesis and tumor progression. Single nucleotide polymorphisms (SNPs) at microRNA-binding sites may change messenger RNA target gene function, thus leading to cancer susceptibility and tumor progression. In this study of 1584 cervical cancer cases and 1394 cancer-free female controls, we investigated associations between three potentially functional SNPs in *TNFAIP8* family genes and cervical cancer risk as well as platinum resistance and clinical outcomes in Eastern Chinese women. We found that the *TNFAIP8*-rs11064 variant GG genotype was associated with an increased risk of cervical cancer compared with AA/AG genotypes (adjusted odds ratio = 2.16, 95% confidence interval = 1.16–4.03, $P = 0.015$). Further *in vitro* and *ex vivo* functional experiments demonstrated that the *TNFAIP8*-rs11064 variant G allele weakened the binding affinity of *miR-22* to the *TNFAIP8* 3'-untranslated region (UTR) in four cancer cell lines, resulting in increased production of the TNFAIP8 protein in the patients' cervical tissues. In the survival subset, the high TNFAIP8 protein expression was significantly associated with both resistance to cisplatin and nedaplatin, recurrence and death from cervical cancer. Taken together, in the absence of information on human papillomavirus (HPV) infection, the *TNFAIP8*-rs11064 SNP may function by affecting the affinity of *miR-22* binding to the 3'-UTR of *TNFAIP8* and regulating TNFAIP8 expression, thus contributing to cervical cancer risk. Additionally, the increased TNFAIP8 protein expression may predict platinum resistance and clinical outcomes in cervical cancer patients. Larger, prospective studies with detailed HPV infection data are warranted to validate our findings.

Abbreviations: BMI, body mass index; CI, confidence interval; FPRP, false-positive report probability; HPV, human papillomavirus; IHC, immunohistochemistry; LN, lymph node; LVSI, lympho-vascular space invasion; MFE, minimum free energy; mRNA, messenger RNA; miRNA, microRNA; OR, odds ratio; TNFAIP8, tumor necrosis factor- α -induced protein 8; SCC, squamous cell carcinoma; SNP, single nucleotide polymorphism; UTR, untranslated region.

Introduction

The tumor necrosis factor- α -induced protein 8 (TNFAIP8) family is a newly identified and less well-characterized group of proteins that are important for maintaining immune homeostasis and inhibiting apoptosis (1). The mammalian TNFAIP8 family consists of TNFAIP8 (also named as SCC-S2, NDED), TNFAIP8-like 1 (TNFAIP8L1, TIPE1), TNFAIP8L2 (TIPE2) and TNFAIP8L3 (TIPE3) (1). These proteins share high degrees of sequence homology and are found to be involved in the process of proliferation, inflammation and cell death (2).

Several studies have found that TNFAIP8 and TNFAIP8L1 act as antiapoptotic and pro-oncogenic signaling molecules and play important roles in immunity, oncogenesis and tumor progression (2–4). TNFAIP8L2 is an essential negative regulator of both innate and adaptive immunity and is involved in the development of inflammatory diseases (5,6), whereas little is known about TNFAIP8L3. Previous data have suggested that TNF stimulation and the activation of the nuclear factor-kappaB pathway can upregulate messenger RNA (mRNA) expression levels of *TNFAIP8* in head and neck squamous cell carcinoma (SCC) cell lines (7). Moreover, the overexpression of *TNFAIP8* is correlated with cancer progression and poor prognosis in several kinds of human cancers (8,9). However, the physiological and pathophysiological roles of the *TNFAIP8* family genes in cervical carcinogenesis and tumor growth are not fully understood.

Cervical cancer is the second most commonly diagnosed cancer and the second leading cause of cancer death in women in the developing countries (10). It is well known that persistent infection with an oncogenic high-risk human papillomavirus (HPV) type is the primary cause of cervical cancer (11). Because host immune response plays a role in eliminating the viral infection and preventing progression to cervical cancer (12), in which *TNFAIP8* family genes may be activated and involved in the development and prognosis of cervical cancer.

A number of studies have demonstrated that deregulation of microRNAs (miRNAs) is involved in cell differentiation, proliferation, apoptosis and carcinogenesis (13). MiRNAs are single-stranded 21–23 nucleotide long endogenous non-coding RNAs that may regulate thousands of target mRNAs by binding to their 3'-untranslated regions (UTRs) (14). This process results in either the degradation of target mRNAs or repression of their translation, and these targets can be implicated in the regulation of almost all biological processes (15). Several recent studies have indicated that single nucleotide polymorphisms (SNPs) at miRNA-binding sites can remarkably alter the biogenesis and/or function of the corresponding miRNAs and thus contribute to the development of human cancers (16,17) and platinum resistance (18). To date, the role of miRNA and functional variants in *TNFAIP8* family genes has been poorly characterized. More importantly, several potentially functional SNPs of the *TNFAIP8* family genes are predicted to be located at the miRNA-binding sites (Supplementary Table I, available at *Carcinogenesis* Online), which allows us to explore their associations with cervical cancer risk and clinical outcomes. Meanwhile, we speculated that these variations might predict clinical outcomes by affecting the response of cancer cells to platinum drugs.

Therefore, we performed a large case-control study to test the hypothesis that functional variants at the miRNA-binding sites of the *TNFAIP8* family genes are associated with cervical cancer risk, platinum resistance and clinical outcomes. We searched and selected the following three common (minor allele frequency > 5%) potentially functional SNPs: *TNFAIP8*-rs11064, *TNFAIP8*-rs3813308 and *TNFAIP8L1*-rs1060555. To address the functional relevance of these selected SNPs, we also investigated the associations of their genotypes with expression levels of both mRNA and protein as well as the allelic functionality by the luciferase reporter assay.

Materials and methods

Study subjects

The study population consisted of 1584 cervical cancer patients and 1394 cancer-free female controls. The patients had been operated between February 2008 and March 2011 in Fudan University Shanghai Cancer Center. All tumors were histopathologically confirmed as primary cancer of the cervix independently by two gynecologic pathologists as routine diagnosis at Fudan University Shanghai Cancer Center. The controls were enrolled from women who had come to the Outpatient Department of Breast Surgery at Fudan University Shanghai Cancer Center for breast cancer screening and agreed to participate in this study. These female controls, with the selection criteria including no individual history of cancer, were frequency matched to the cases on age (\pm within 5 years) and residential regions. All subjects were unrelated ethnic Han Chinese and residents in the Eastern China. During an in-person survey, all potential subjects were interviewed to identify their willingness to participate in research studies and to collect their demographic and risk factor information. Approximate response rates for the cases and controls were 95% and 95%, respectively. Because most Chinese women included in this study were non-smokers and non-drinkers, our study populations were restricted to women who did not smoke cigarettes or drink alcohol. For the cases, the detailed clinico-pathologic information was extracted from the patients' electronic database, as described previously (19), including tumor histology (20), FIGO stage (International Federation of Gynecology and Obstetrics, 2009), tumor size (i.e. the size of the primary tumor was the largest tumor diameter), pelvic lymph node (LN) metastasis, lympho-vascular space invasion (LVSI) and depth of cervical stromal invasion (Supplementary Table II, available at *Carcinogenesis* Online). Each participant provided a one-time 10 ml of venous blood sample (after the diagnosis and before the initiation of treatment for the cases), which were kept frozen till DNA extraction for genotyping.

In the survival subset, we included 148 cervical cancer patients, who were histopathologically confirmed as SCC and underwent radical hysterectomy plus pelvic lymphadenectomy. The detailed treatment protocol has been described elsewhere (21). Briefly, 3 weeks after radical surgery, the patients with at least two high-risk factors, such as positive pelvic LN metastasis and/or large tumor size and/or positive LVSI and/or positive surgical margin and deep cervical stromal invasion, were treated with concurrent chemoradiation therapy that included the pelvic irradiation (45 Gy) with weekly cisplatin (30 mg/m² cisplatin and 45 mg/m² paclitaxel). We then followed up every 3 months for the first 2 years, every 6 months for the next 2 years and annually for the following years thereafter. Recurrence was defined as the outcome of disease after a disease-free interval of more than 3 months after primary treatment and grouped by different sites as follows: locally (i.e. vaginal apex), regionally (i.e. pelvic sidewall) or distantly (i.e. liver or lung) (Supplementary Table III, available at *Carcinogenesis* Online). Progression-free survival and overall survival times were calculated from the date of first surgery to the date of recurrence and death, respectively. Patients without progression or died from other causes were censored at their last date of record.

All samples were obtained from tissue bank of Fudan University Shanghai Cancer Center. The research was approved by the institutional review board of Fudan University Shanghai Cancer Center, and a written informed consent was obtained from all recruited individuals.

Identification and in silico analysis of potential functional variants

We evaluated all SNPs in the 3'-UTR of the four *TNFAIP8* family genes with a minor allele frequency of at least 5% in Han Chinese populations, based on the dbSNP database of National Center for Biotechnology Information (<http://www.ncbi.nlm.nih.gov/projects/SNP>) and the International HapMap Project database (<http://hapmap.ncbi.nlm.nih.gov>). Supplementary Table I, available at *Carcinogenesis* Online, showed that there were three and seven SNPs in the *TNFAIP8* and *TNFAIP8L1* genes, respectively, but none was found in 3'-UTRs of *TNFAIP8L2* and *TNFAIP8L3*. Of these 10 SNPs, two (i.e. rs1045241 and rs1045242) were in high linkage disequilibrium with another one (i.e. rs11064) by using an r^2 threshold of 0.8, and six were not predicted as potentially functional SNPs by SNP function prediction (FuncPred) software from National Institute of Environmental Health Sciences (<http://snpinfo.nih.gov>). As a result, we selected one *TNFAIP8* SNP [rs11064 (3'-UTR 312) A>G (Figure 1A)] and one *TNFAIP8L1* SNP [rs1060555 (3'-UTR 380) C>G]. Additionally, we added one more potentially functional SNP in the 5'-flanking of the *TNFAIP8* gene as a reference SNP (i.e. *TNFAIP8*-rs3813308 C>G). Therefore, this study included three SNPs of *TNFAIP8* family genes, which capture 24 other untyped SNPs (Supplementary Figure 1A and B, available at *Carcinogenesis* Online).

We then performed miRBase (<http://www.mirbase.org/>), miRanda (<http://www.microrna.org/microrna/releaseNotes.do>) and TargetScanHuman 6.2 (<http://www.targetscan.org/>) to predict miRNA targets. The RNAfold online tool (<http://rna.tbi.univie.ac.at/>) was used to estimate the RNA secondary structure based on minimum free energy (MFE) values.

DNA extraction and genotyping

Genomic DNA was obtained from the whole blood, and the Taqman method was performed for genotyping, as described previously (22). Four negative controls (without DNA template), duplicated positive controls and eight repeat samples were included in each 384-well plate for the quality control. As a result, the mean genotyping rate was 98.9%, and the discrepancy rate in all positive controls (i.e. duplicated samples, overlapping samples from previous studies and samples randomly selected to be sequenced) was <0.1%.

Cloning and site-directed mutagenesis

The 509bp fragment of human *TNFAIP8* 3'-UTR containing the rs11064 A allele was amplified from a homozygous human genomic DNA sample (Supplementary Table IV, available at *Carcinogenesis* Online). After purification, the PCR product was cloned into the psiCHECKTM-2 vector (Promega, Madison, WI) using the XhoI and NotI restriction sites located at the 3' to the *Renilla* luciferase translational stop codon. The rs11064 G allele was generated with the QuickChange Site-Directed Mutagenesis kit (Stratagene, La Jolla, CA) according to the manufacturer's protocol. This method was used to avoid non-specific cloning during the construction of mutant libraries (23). All constructs used in this study were verified by direct sequencing, and the generated reporter vectors were named psiCHECK2:rs11064A and psiCHECK2:rs11064G, respectively (Figure 1B).

Quantitative PCR, transient transfection and luciferase reporter assay

Four cancer cell lines, the cervical adenocarcinoma HeLa and SCC SiHa cell lines, lung cancer cell line A549 and colorectal cancer cell line SW480, were used for the luciferase reporter assay. All these four cell lines were obtained from the American Type Culture Collection. Morphology and growth curve were recorded regularly to ensure the maintenance of phenotypes. Cells were used for no more than 3 months after resuscitation. They were cultured in Dulbecco's modified Eagle's medium [(Cat# L0103; Biowest, Nuaille, France) for HeLa and SiHa], RPMI 1640 medium [(Cat# L0498; Biowest for A549) and Leibovitz's L-15 medium [(Cat#L4386, Sigma-Aldrich Co., St Louis, MO) for SW480], supplemented with 10% fetal bovine serum (Cat# S1810; Biowest) at 37°C, humidified incubator supplied with 5% CO₂. We first detected the baseline levels of the *TNFAIP8* mRNA expression for the four cell lines. Total RNA was extracted from the cultured cells, and the SYBR Green fluorescent-based assay (TaKaRa Bio, Shiga, Japan) was performed for the quantitative PCR (Supplementary Table IV, available at *Carcinogenesis* Online), as described previously (22). We evaluated readout values by normalizing the copy number of *TNFAIP8* to that of β -actin and calculated the relative expression of *TNFAIP8* mRNA by using $2^{-\Delta\Delta CT}$ ($\Delta\Delta CT = \text{Avg. } TNFAIP8 \text{ CT} - \text{Avg. } \beta\text{-actin CT}$) (24).

To conduct the luciferase reporter assay, a total of 2×10^5 cells from each cell line were plated onto each well of six-well plates. After an overnight incubation, cells were co-transfected with Lipofectamine2000 (Invitrogen, Carlsbad, CA). Each co-transfection reaction contained 200 pmol *miR-22* (GenePharma Co., Ltd, Shanghai, China) with 2 μ g of the psiCHECK2:control, psiCHECK2:rs11064A or psiCHECK2:rs11064G plasmid DNA. Forty-eight hours after transfection, cells were washed and lysed with 500 μ l passive lysis buffer (Promega), of which 20 μ l lysed cells were used for the quantification of both *Firefly* and *Renilla* luciferase activities by the Dual-Luciferase Reporter Assay System (Cat#E1910; Promega) and SynergyTM 4 Multi-Mode Microplate Reader (BioTek, Winooski, VT) according to the manufacturers' protocols. The relative luciferase activity = *Renilla*/*Firefly* luciferase activity. For the other lysed cells left, we evaluated mRNA expression levels of the *Renilla*/*TNFAIP8* 3'-UTR region by normalizing to that of β -actin using the quantitative PCR assay (Supplementary Table IV, available at *Carcinogenesis* Online).

Genotype and mRNA expression data of TNFAIP8 from the HapMap database

The data on *TNFAIP8*-rs11064 genotypes and *TNFAIP8* mRNA expression levels were both available for 270 HapMap individuals, including 45 Chinese subjects, by the SNPexp online tool (<http://app3.titan.uio.no/biotools/help.php?app=snpexp>) (25). We used Student's *t*-test and analysis of variance test to evaluate the differences in the relative mRNA expression levels among different genotype groups, as described previously (26).

TNFAIP8 protein expression levels by TNFAIP8 genotypes in the target tissues

The *TNFAIP8* protein expression was performed by the immunohistochemistry (IHC) assay on 5 μ m thick tissue sections prepared from formalin-fixed, paraffin-embedded tissue from the constructed 10 \times 12 tissue microarray block using the antibody against *TNFAIP8* (sc-82054, goat polyclonal IgG, 1:50 dilution; Santa Cruz Biotechnology, Santa Cruz, CA) and SABC (goat IgG) detection kit (Cat#SA1023; BOSTER, Wuhan, China). Two tissue cores were obtained for each case. A known positive sample was included as positive control. For the negative control, the primary antibody was replaced with

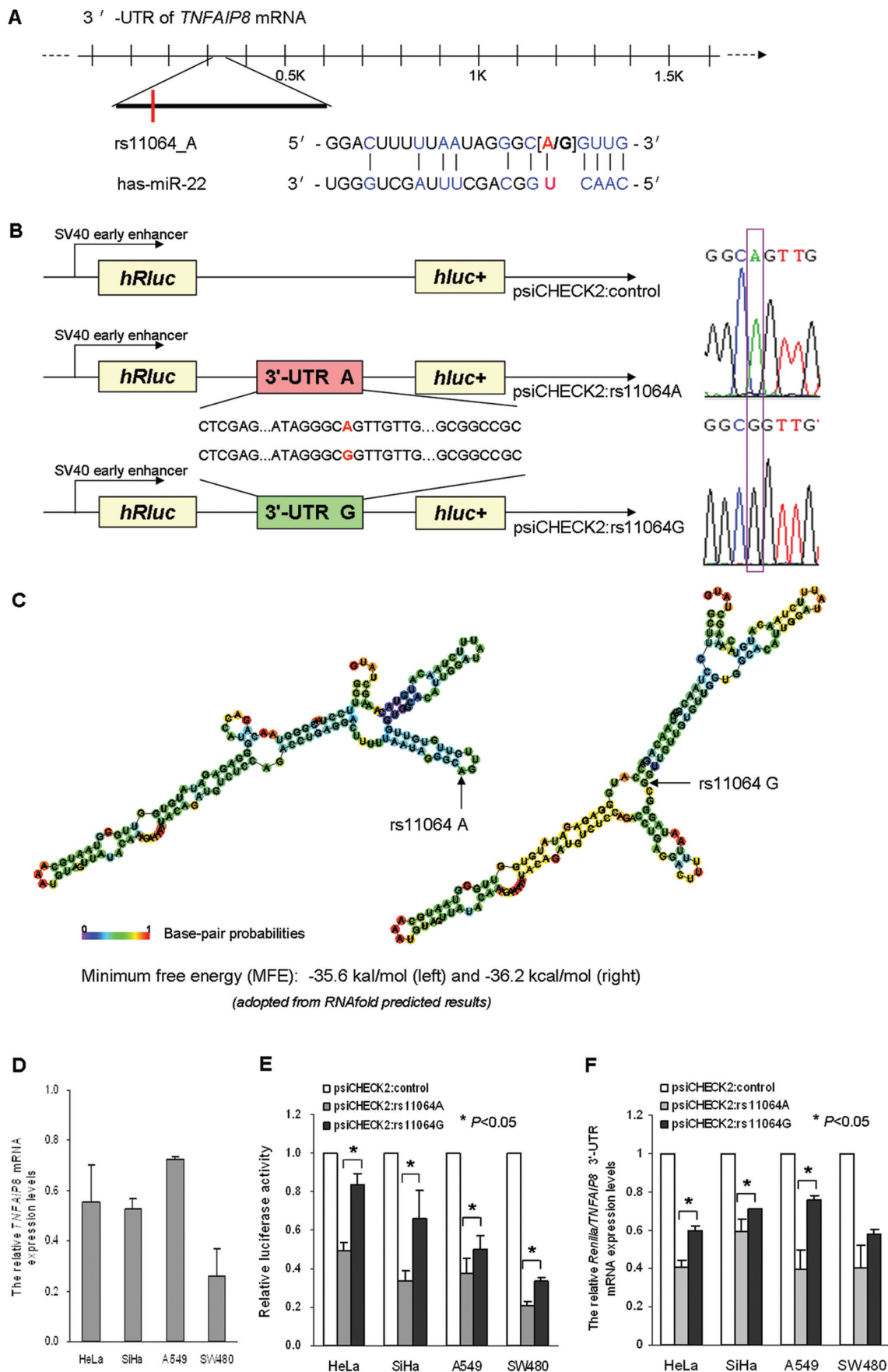


Fig. 1. The *TNFAIP8*-rs11064 A>G SNP contributes to the binding affinity of *miR-22* to the *TNFAIP8* 3'-UTR. (A) The rs11064 SNP is located at the *TNFAIP8* 3'-UTR, which is also at the miRNA-binding site with the A allele perfectly matching the corresponding U allele in *miR-22*. (B) Schematic drawing of the

non-immune goat serum. The IHC staining results were independently scored by two researchers (T-Y.S. and Q-X.L.), who were blinded to patient information using a scoring system based on both the percentage of positive tumor cells and staining intensity, as described previously (27). The assessment of the protein expression was defined as low ($\leq 3+$) and high ($> 3+$) levels, and for the cores that were uninterpretable because of tissue loss or lack of tumor cells, a score of Not Applicable was assigned.

Cell isolation and the 3-(4,5-dimethylthiazole-2-yl)-2,5-diphenyl tetrazolium bromide assay

Histopathologically confirmed fresh tumor tissues obtained from patients by surgery were cut into pieces smaller than 5×5 mm and suspended in the RPMI 1640 medium supplied with 15% fetal bovine serum at room temperature. Suspended tumor cells were poured over a 150 μ m sterile steel mesh placed in the dish. Percoll discontinuous gradient centrifugation with 1000 r.p.m. was used to separate and purify tumor cells (28). Tumor cells were then collected and resuspended at a concentration of 1×10^5 viable cells/ml and cultured in 96-well microplates at 37°C in a 5% CO₂ incubator. On day 2, platinum drugs (cisplatin, carboplatin, nedaplatin and oxaliplatin with a final concentration of 100, 200, 100 and 120 ng/ml, respectively) were added into the culture system for 48 h, as described previously (29). The measurements were performed in duplicate. For each patient, tumor cells without the drugs were cultured as negative assay controls in the meantime. At the end of cultivation, the medium was removed and cells were incubated with 1 mg/ml thiazolyl blue tetrazolium bromide (Sigma–Aldrich) at 37°C for 4 h. The formazan crystals were dissolved in solution buffer (10% sodium dodecyl sulfate, 5% isobutanol and 0.012 mol/l HCl) overnight, and OD_{570 nm} was measured by Bio-Rad 550 microplate reader (Bio-Rad, Hercules, CA). The inhibition rate = $(1 - \text{OD}_{570 \text{ nm}} / \text{OD}_{570 \text{ nm}} \text{ control}) \times 100\%$.

Statistical analysis

Hardy–Weinberg Equilibrium was tested by χ^2 test for each SNP. The differences in selected variables between cervical cancer cases and controls, as well as the distributions of TNFAIP8 protein expression levels among different TNFAIP8 genotypes, were evaluated by the Pearson's χ^2 test. Logistic regression models were used to evaluate associations of selected SNPs with cervical cancer risk and with protein expression levels by computing the odds ratios (ORs) and their 95% confidence intervals (CIs). These analyses were performed with or without adjustment for age (in years), age of primiparity, menopause status and body mass index (BMI) (30). These associations were also stratified by demographic and clinico-pathologic variables. We applied the PROC HAPLOTYPE procedure in SAS software to infer haplotype frequencies among the two TNFAIP8 SNPs based on their observed genotypes. For all significant genetic effects observed in this study, we calculated the false-positive report probability (FPRP) with prior probabilities of 0.0001, 0.001, 0.01, 0.1 and 0.25 to test for false-positive associations, and a $P < 0.2$ was considered noteworthy (31). Shapiro–Wilk test was used to evaluate normal distributions for continuous variables. We performed Student's *t*-test or Wilcoxon test to compare continuous variables between two groups, and used analysis of variance or Kruskal–Wallis test to compare continuous variables among three or four groups. For survival analysis, Kaplan–Meier curve and log rank test, as well as univariate and multivariate Cox proportional hazards regression analyses, were conducted. All statistical analyses were performed with SAS software (version 9.1; SAS Institute, Cary, NC), unless stated otherwise. All *P* values were two-sided with a significance level of $P < 0.05$.

Results

Demographic characteristics of the study population

The final analysis included 1567 cases and 1380 controls. As shown in Supplementary Table II, available at *Carcinogenesis* Online, there were no significant differences in the distributions of age between the cases and the controls with similar mean ages of 45.8 (± 9.8) and 46.2 (± 8.8) years, respectively ($P = 0.132$). Among these 1567 cases, there

were 1240 cases with SCC, whose distribution of age was similar to that of the controls. However, there were significant differences in age of primiparity, menopausal status and BMI between cases and controls (all $P < 0.001$ for all cases and for cases with SCC only, respectively), with the cases more likely to be premenopausal, thinner and younger at primiparity than the controls. Thus, we further adjusted these variables for any residual confounding effect in later multivariate logistic regression analyses.

Association between SNPs and cervical cancer risk

The genotype frequencies of the three selected SNPs and their associations with cervical cancer risk are summarized in Table I. All the observed genotype distributions among the controls agreed with Hardy–Weinberg Equilibrium ($P = 0.057$, 0.637 and 0.593 for TNFAIP8-rs11064, TNFAIP8-rs3813308 and TNFAIP8LI-rs1060555, respectively). Compared with the AA genotype and AA/AG genotypes, the TNFAIP8-rs11064 variant GG genotype was found to be significantly associated with an increased risk of cervical cancer (adjusted OR = 2.15 and 2.16, 95% CI = 1.15–4.02 and 1.16–4.03, $P = 0.016$ and 0.015, respectively). However, this association was not observed for the TNFAIP8-rs3813308 and TNFAIP8LI-rs1060555 SNPs or for the haplotype analysis of the two TNFAIP8 SNPs (Supplementary Table V, available at *Carcinogenesis* Online). When combining these two TNFAIP8 SNPs and assuming a recessive genetic model, we found that those women who carried two TNFAIP8 variant genotypes had a 4.73-fold increased risk (95% CI = 1.56–14.29, $P = 0.006$) of cervical cancer, compared with those who carried one or less variant genotype (Table I).

In the stratified analysis, under a recessive genetic model, we found that the significantly increased risk of cervical cancer associated with the TNFAIP8-rs11064 GG genotype was more evident in younger (≤ 24 years, $P = 0.038$) or thinner (BMI < 25 kg/m², $P = 0.012$) women and in subgroups of FIGO stage I, tumor size (< 4 cm), negative pelvic LN, negative LVSI and depth of cervical stromal invasion $\leq 1/2$ (Supplementary Table VI, available at *Carcinogenesis* Online). However, homogeneity tests suggested that there was no difference in risk estimates between subgroups of the strata. Meanwhile, we observed a borderline-significant locus–locus interaction between the two selected TNFAIP8 SNPs (i.e. rs11064 and rs3813308; adjusted OR = 3.49, 95% CI = 0.94–13.04, $P = 0.063$).

We then calculated FPRP values for all observed significant associations. When the assumption of prior probability was 0.25, the association with TNFAIP8-rs11064 GG genotypes was noteworthy for the subgroups of tumor size < 4 cm and negative LN metastasis (FPRP = 0.143 and 0.189, respectively) as well as TNFAIP8LI-rs1060555 GG genotypes for the women who were of younger age at primiparity (≤ 24 years, FPRP = 0.138).

MiR-22 differentially regulates TNFAIP8 mRNA expression through allelic variants of rs11064

Because the mRNA secondary structure is critical for mRNA–miRNA interactions (32), we further explored whether the TNFAIP8-rs11064 SNP in the 3'-UTR of TNFAIP8 could alter the local secondary structure of the TNFAIP8 mRNA based on the MFE value. Using the RNAfold online tool and inputting 162-nucleotide long DNA sequence of the TNFAIP8 3'-UTR containing the rs11064 locus, we

← luciferase reporter vectors. The control psiCHECK2 luciferase vector (top) and psiCHECK2 vectors contain a partial TNFAIP8 3'-UTR sequence with either the A (middle) or G (bottom) allele at the rs11064 locus. The graphs on the right side show sequencing results for A and G alleles. (C) The predicted secondary structure of the TNFAIP8 mRNA. The secondary structures of the TNFAIP8 3'-UTR were predicted by inputting two 162 nucleotide long DNA sequences centering rs11064 into RNAfold, with either the A (left) or G (right) allele. The figures and the values of MFE were generated by RNAfold (<http://ma.tbi.univie.ac.at>). (D) The TNFAIP8 mRNA was expressed in the four cancer cell lines with relatively higher levels in A549 and SiHa, and lower levels in SW480 and HeLa. (E) Luciferase reporter assay. For each transfected cell line, compared with the psiCHECK2:rs11064G vector, the psiCHECK2:rs11064A vector showed a significantly decreased level of the relative *Renilla/Firefly* luciferase activity (Student's *t*-test, $P < 0.001$ for HeLa, SiHa and SW480; $P = 0.009$ for A549, respectively); (F) Quantitative PCR assay. For each transfected cell line, compared with the psiCHECK2:rs11064G vector, the psiCHECK2:rs11064A vector showed a decreased trend of *Renilla/TNFAIP8* 3'-UTR mRNA expression levels (Student's *t*-test, $P = 0.002$, 0.035, 0.004 and 0.062 for HeLa, SiHa, A549 and SW480, respectively).

Table I. Associations of *TNFAIP8* and *TNFAIP8LI* genotypes with the risk of cervical carcinoma

Variant genotypes	Cases (N = 1567)	Controls (N = 1380)	P ^a	Crude OR (95% CI)	P	Adjusted OR (95% CI) ^b	P ^b
<i>TNFAIP8</i> -rs11064							
AA	1178 (75.2)	1039 (75.3)	0.015	1.00		1.00	
AG	350 (22.3)	326 (23.6)		0.95 (0.80–1.13)	0.535	0.98 (0.82–1.17)	0.820
GG	39 (2.5)	15 (1.1)		2.29 (1.26–4.18)	0.007	2.15 (1.15–4.02)	0.016
Additive model				1.07 (0.92–1.24)	0.395	1.09 (0.93–1.27)	0.314
Dominant model			0.943	1.01 (0.85–1.19)	0.943	1.03 (0.87–1.23)	0.718
Recessive model			0.005	2.32 (1.27–4.23)	0.006	2.16 (1.16–4.03)	0.015
<i>TNFAIP8</i> -rs3813308							
CC	416 (26.6)	337 (24.4)	0.415	1.00		1.00	
CG	754 (48.1)	681 (49.4)		0.90 (0.75–1.07)	0.230	0.90 (0.74–1.08)	0.251
GG	397 (25.3)	362 (26.2)		0.89 (0.73–1.09)	0.253	0.88 (0.71–1.09)	0.254
Additive model				0.94 (0.85–1.04)	0.253	0.94 (0.85–1.05)	0.255
Dominant model			0.186	0.89 (0.76–1.06)	0.188	0.89 (0.75–1.06)	0.200
Recessive model			0.579	0.95 (0.81–1.13)	0.578	0.95 (0.80–1.13)	0.557
<i>TNFAIP8LI</i> -rs1060555							
CC	867 (55.3)	757 (54.9)	0.354	1.00		1.00	
CG	609 (38.9)	525 (38.0)		1.01 (0.87–1.18)	0.870	0.98 (0.84–1.15)	0.831
GG	91 (5.8)	98 (7.1)		0.81 (0.60–1.10)	0.172	0.84 (0.61–1.16)	0.290
Additive model				0.95 (0.85–1.07)	0.436	0.95 (0.84–1.08)	0.410
Dominant model			0.797	0.98 (0.85–1.14)	0.797	0.96 (0.82–1.12)	0.612
Recessive model			0.152	0.81 (0.60–1.08)	0.152	0.85 (0.62–1.16)	0.300
Combined effects of two risk genotypes of <i>TNFAIP8</i> by the recessive model							
0	1152 (73.5)	1007 (73.0)	0.006	1.00		1.00	
1	394 (25.1)	369 (26.7)		0.93 (0.79–1.10)	0.413	0.92 (0.78–1.10)	0.372
2	21 (1.3)	4 (0.3)		4.59 (1.57–13.41)	0.005	4.63 (1.53–14.01)	0.007
				$P_{\text{trend}} = 0.769$		$P_{\text{trend}}^b = 0.877$	
0–1	1546 (98.7)	1376 (99.7)	0.002	1.00		1.00	
2	21 (1.3)	4 (0.3)		4.67 (1.60–13.64)	0.005	4.73 (1.56–14.29)	0.006

The results are shown in bold, if $P < 0.05$.

^a χ^2 test for genotype distributions between cases and controls.

^bAdjusted for age, age at primiparity, menopausal status and BMI in logistic regression models.

found that the MFE changed from -35.6 to -36.2 kcal/mol, when the rs11064 allele changed from A to G (Figure 1C).

Given that rs11064 A>G was located at the miRNA-binding site of *TNFAIP8* with the A allele perfectly matching the corresponding U allele of *miR-22* (Figure 1A), we then performed the luciferase reporter assay to determine whether *miR-22* could differentially regulate the *TNFAIP8* mRNA expression through different rs11064 alleles. Baseline levels of the *TNFAIP8* mRNA expression in the four cancer cell lines are shown in Figure 1D, with relatively higher levels in A549, medium levels in HeLa and SiHa, and lower levels in SW480. For each cell line, the relative luciferase activities and mRNA expression levels of the two test groups (i.e. psiCHECK2:rs11064A and psiCHECK2:rs11064G) were normalized by those of control groups. We found a significantly decreased level of the relative luciferase activity in the psiCHECK2:rs11064A group compared with the psiCHECK2:rs11064G group (Student's *t*-test, $P < 0.001$ for HeLa, SiHa and SW480; $P = 0.009$ for A549, respectively; Figure 1E); likewise, a decreased trend of *Renilla/TNFAIP8* 3'-UTR mRNA expression levels was observed in the psiCHECK2:rs11064A group, compared with the psiCHECK2:rs11064G group (Student's *t*-test, $P = 0.002$, 0.035, 0.004 and 0.062 for HeLa, SiHa, A549 and SW480, respectively; Figure 1F).

Association between the *TNFAIP8*-rs11064 SNP and expression levels of the *TNFAIP8* mRNA from the HapMap database

We evaluated 270 HapMap individuals for the association between variants and mRNA expression of *TNFAIP8* based on the SNPexp online database available to us. There were 167 AA, 80 AG and 17 GG carriers for the *TNFAIP8*-rs11064 SNP, of which 36 AA and 9 AG carriers were Chinese (no GG was observed in this study population). Because *TNFAIP8* mRNA expression levels obtained from the HapMap database followed normal distributions in both all subjects and Chinese subjects (Shapiro–Wilk test, $P = 0.084$ and 0.842, respectively), the G allele was associated with significantly increased levels

of *TNFAIP8* mRNA expression compared with the A allele in both all 264 subjects (i.e. 528 alleles) and 45 Chinese subjects (i.e. 90 alleles) (Student's *t*-test, $P = 0.021$ and 0.026, respectively; Figure 2A and B).

Associations of *TNFAIP8* SNPs and protein expression with platinum resistance and clinical outcomes in the survival subset

The selected 148 cervical SCC patients for the survival subset analysis did not differ from 1240 cervical SCC patients in most variables of interest (Supplementary Table II, available at *Carcinogenesis* Online); however, three were lost to the follow-up, and one had a score of Not Applicable for the IHC staining of *TNFAIP8*. Therefore, the final analysis included 144 patients with SCC of the cervix, of which 115 cases received concurrent cisplatin and radiation therapy after surgery. The median follow-up period was 35 months (range 24–40).

In the target tissues, there were 83 and 61 cases with high and low expression of *TNFAIP8*, respectively. All the three *TNFAIP8*-rs11064 variant GG carriers had high levels of *TNFAIP8* protein expression. Overall, patients who carried the rs11064 variant G allele had a significantly higher expression level of *TNFAIP8* than those who carried the rs11064 A allele (χ^2 test, $P = 0.012$; adjusted OR = 3.94, 95% CI = 1.28–12.17, $P = 0.017$; Figure 2C, Table II).

We then investigated associations of both *TNFAIP8* SNPs and protein expression with platinum resistance and clinical outcomes. Platinum-inhibition rates by the 3-(4,5-dimethylthiazole-2-yl)-2,5-diphenyl tetrazolium bromide assay were conducted to evaluate platinum resistance *in vitro*. We found that the four platinum drugs showed a significant difference in inhibiting cervical cancer cells (Kruskal–Wallis test, $P < 0.001$), with higher inhibition rates in cisplatin and nedaplatin. However, no significant difference was observed between cisplatin and nedaplatin groups (Wilcoxon test, $P = 0.312$; Supplementary Figure 2, available at *Carcinogenesis* Online). Although we did not observe any associations between *TNFAIP8* SNPs and inhibition rates of the four platinum drugs, the high expression level of *TNFAIP8* was significantly associated with poor response of cervical cancer cells to

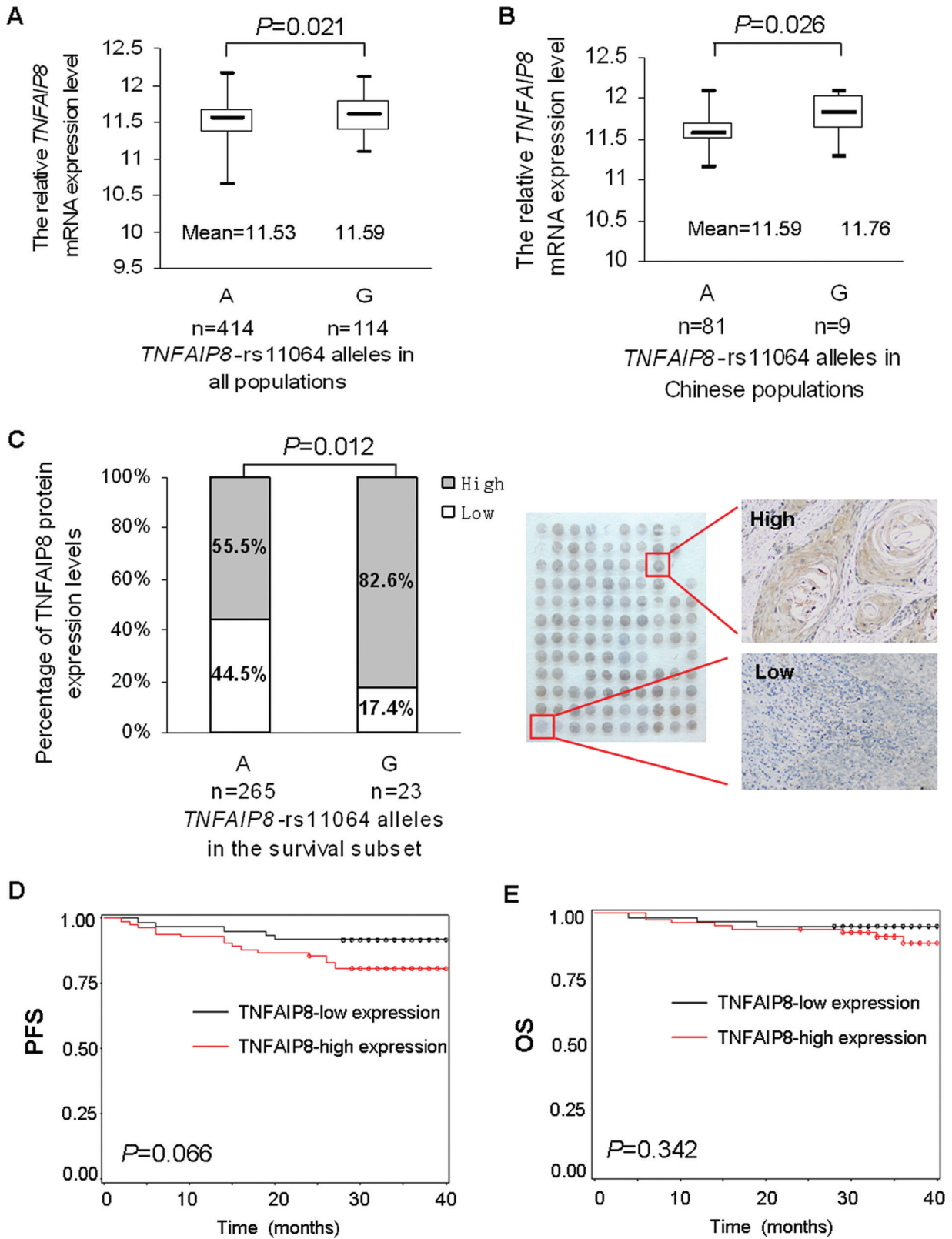


Fig. 2. Differential expression of *TNFAIP8* mRNA and protein by different rs11064 variant alleles. The relative *TNFAIP8* mRNA expression levels by rs11064 alleles were obtained from HapMap for (A) all 270 individuals and (B) the 45 Han Chinese in Beijing (CHB) individuals (<http://app3.titan.uio.no/biotools/help.php?app=snpexp>). Individuals who carry rs11064 G allele had a significantly increased level of *TNFAIP8* mRNA expression than those who carry A allele in both all and Chinese subjects (Student's *t*-test, $P = 0.021$ and 0.026 , respectively). (C) *TNFAIP8* protein expression levels were also investigated in the corresponding tissue with IHC for 144 cervical cancer patients who had 288 alleles at Fudan University Shanghai Cancer Center. The rs11064 variant G allele (all three GG patients had high expression levels) was significantly associated with an increased expression level of *TNFAIP8* protein compared with the A allele (c^2 test, $P = 0.012$). The graphs on the right side show representative IHC results. Cervical cancer patients with high expression levels of *TNFAIP8* showed poorer (D) progression-free survival and (E) overall survival than those with low *TNFAIP8* expression levels ($P = 0.066$ and 0.342 , respectively).

cisplatin and nedaplatin (Wilcoxon test, $P = 0.043$ and 0.009 , respectively; Table III).

No significant association between *TNFAIP8* SNPs and survival was observed (Supplementary Table VII, available at *Carcinogenesis* Online), mainly because there were only three homozygous variant GG carriers among the 144 patients. However, consistent with the results of platinum resistance, we found that the patient who had high expression levels of TNFAIP8 showed a decreased trend of progression-free survival and overall survival (log rank test, $P = 0.066$ and 0.342 , respectively; Figure 2D). Further multivariate Cox proportional hazards regression models demonstrated that the TNFAIP8 protein expression was independently associated with recurrence and death (adjusted hazard ratio = 4.10 and 4.48, 95% CI = 1.38–12.15 and 1.02–19.64, $P = 0.011$ and 0.047 , respectively; Supplementary Table VII, available at *Carcinogenesis* Online); in the same multivariate model, we found that highly advanced tumor stage (IIB), large tumor size (≥ 4 cm) and positive LVSI were also independently associated with recurrence, and positive LVSI with death.

Discussion

To the best of our knowledge, this is the first study that has investigated associations of miRNA-binding site SNPs of the *TNFAIP8* family genes with cervical cancer risk, platinum resistance and clinical

outcomes in Eastern Chinese women. Although no significant association between genotypes of the *TNFAIP8*-like genes and cervical cancer risk was observed, we found that the *TNFAIP8*-rs11064 variant GG genotype was associated with an increased risk of cervical cancer. Further genotype–phenotype correlation analyses and additional experiments suggested that this SNP might function by affecting the affinity of *miR-22* binding to the 3'-UTR of *TNFAIP8* and regulating expression levels of the *TNFAIP8* mRNA and TNFAIP8 protein, thus contributing to cervical cancer risk. Moreover, survival analyses of a subset showed a potential effect of TNFAIP8 expression on platinum resistance and clinical outcomes, indicating that functional variants in *TNFAIP8* might be involved in tumor progression and prognosis of cervical cancer by affecting the response of tumor cells to platinum drugs, especially cisplatin and nedaplatin.

TNFAIP8 is one of the *TNFAIP8* family genes that have been less well characterized. *TNFAIP8* is located at chromosome 5q23.1 and encodes a 21 kDa cytosolic protein, which consists of 11 exons and 10 introns and spans ~13.5 kb of genomic DNA. It has been originally identified in a metastatic and radio-resistant primary human head and neck cancer cell line (PCI-06B) (33). Subsequently, several studies have showed that *TNFAIP8* plays important roles in maintaining immune homeostasis and inducing the development and progression of tumors as an oncogene (2–4). Meanwhile, its overexpression could lead to cell proliferation (3). Others reported that TNFAIP8

Table II. Logistic regression analysis of correlation between *TNFAIP8* genotypes and TNFAIP8 protein expression in cervical cancer tissues from 144 patients

<i>TNFAIP8</i> variants	TNFAIP8 protein expression		P^a	Crude OR (95% CI)	P	Adjusted OR (95% CI) ^b	P^b
	High N (%)	Low N (%)					
Alleles							
All cases ($N = 288$)	166 (57.6)	122 (42.4)					
rs11064			0.012				
A	147 (55.5)	118 (44.5)		1.00		1.00	
G	19 (82.6)	4 (17.4)		3.81 (1.26–11.51)	0.018	3.94 (1.28–12.17)	0.017
rs3813308			0.394				
C	86 (60.1)	57 (39.9)		1.00		1.00	
G	80 (55.2)	65 (44.8)		0.82 (0.51–1.30)	0.394	0.78 (0.48–1.27)	0.315

The results are shown in bold, if $P < 0.05$.

^a χ^2 test for genotype distributions between high and low levels of TNFAIP8 protein.

^bAdjusted for age, age at primiparity, menopausal status and BMI in logistic regression models.

Table III. Variants and TNFAIP8 protein expression as predictors of response to platinum agents in the survival subset

Variables	Cases N (%)	Cisplatin		Carboplatin		Nedaplatin		Oxaliplatin	
		Median \pm SE (%)	P^a	Median \pm SE (%)	P^a	Median \pm SE (%)	P^a	Median \pm SE (%)	P^a
All patients ^b	144 (100)	81.6 \pm 2.1		35.7 \pm 2.5		77.7 \pm 2.1		55.8 \pm 2.6	
<i>TNFAIP8</i> -rs11064 ^c			0.603		0.964		0.567		0.928
A	265 (92.2)	81.5 \pm 1.6		35.0 \pm 1.9		77.8 \pm 1.6		56.2 \pm 1.9	
G	23 (7.8)	85.1 \pm 5.6		38.0 \pm 5.7		71.1 \pm 5.2		48.7 \pm 6.6	
<i>TNFAIP8</i> -rs3813308 ^c			0.869		0.632		0.315		0.556
C	143 (50)	81.8 \pm 2.2		36.4 \pm 2.6		78.3 \pm 2.0		57.9 \pm 2.5	
G	145 (50)	79.6 \pm 2.1		34.2 \pm 2.5		74.5 \pm 2.2		48.9 \pm 2.6	
<i>TNFAIP8</i> LI-rs1060555 ^d			0.277		0.422		0.937		0.275
C	209 (74.8)	81.5 \pm 1.7		35.0 \pm 2.1		78.2 \pm 1.7		51.0 \pm 2.2	
G	71 (25.2)	84.9 \pm 3.3		36.7 \pm 3.4		77.6 \pm 3.3		62.0 \pm 3.7	
TNFAIP8 protein expression levels			0.043		0.729		0.009		0.783
Low	61 (42.9)	88.0 \pm 3.5		29.7 \pm 3.6		85.5 \pm 3.2		47.2 \pm 4.2	
High	83 (57.1)	77.6 \pm 2.6		44.9 \pm 3.5		71.2 \pm 2.8		57.9 \pm 3.2	

The results are shown in bold, if $P < 0.05$.

^aWilcoxon test for platinum-inhibition rates between different groups.

^bOf the 148 patients, three were lost to the follow-up, and one had a score of Not Applicable for the IHC staining of TNFAIP8.

^cAll 144 patients with 288 alleles.

^dFour patients were unsuccessfully genotyped for rs1060555.

contains a death effector domain and thus may cause the inhibition of caspase-mediated apoptosis (34). For example, the downregulation of *TNFAIP8* alone was sufficient to resist glucocorticoid-induced apoptosis (35). In cancers of the head and neck, breast, lung and esophagus, expression levels of *TNFAIP8* in cancer tissues were much higher than those in the matched normal adjacent tissues (3,8,9,34). Several studies reported that *TNFAIP8* expression levels were associated with LN metastasis and poor prognosis and that it may be a potential therapeutic target for human cancers (8,9). However, its association with platinum resistance was never reported.

In this study, the *TNFAIP8*-rs11064 SNP was found to be associated with cervical cancer risk in Chinese women, with the variant G allele as a risk allele. By using the linkage disequilibrium analysis, the two studied *TNFAIP8* SNPs (i.e. rs11064 and rs3814408) captured 16 other untyped SNPs, of which the rs1045241 was in high linkage disequilibrium with rs11064 ($r^2 = 0.85$; Supplementary Figure 1A, available at *Carcinogenesis* Online). Consistent with our findings, rs1045241T was recently reported to be associated with an increased risk of non-Hodgkin's lymphoma in a Chinese population (36), the only reported study in the literature, to date. Besides, we found that the combined variant genotypes of these two studied *TNFAIP8* SNPs were associated with cervical cancer risk and that there was also a borderline-significant locus-locus interaction between these two SNPs, which provides an additional evidence to support the role of *TNFAIP8* SNPs as an underlying mechanism in the development of cervical cancer.

Studies have demonstrated that miRNAs may function as tumor suppressors and/or oncogenes in many cancers, including cervical cancer (37,38). Importantly, miRNAs can regulate gene expression and participate in gene regulatory networks by the sequence-specific binding to their target mRNAs (32). SNPs located at the miRNA-binding sites may affect these binding processes (39), thus contributing to cancer development and possibly platinum resistance (18). To date, few studies have investigated the effect of SNPs at miRNA-binding sites on cervical cancer risk, two of which have dealt with two SNPs located in miRNA target genes (i.e. *LAMB3*-rs2566 and *BCL2*-rs3744935) (40,41). However, these studies had relatively small sample sizes (<700 cases), and none of these studies investigated genetic variations of *TNFAIP8*. In this study, we found that the *TNFAIP8*-rs11064G was associated with an increased cervical cancer risk, which was biologically plausible because the G allele associated with the risk may be due to higher expression levels of the gene and subsequently increased apoptotic potential of the cells, given that *TNFAIP8* may be an oncogene (3). However, the *TNFAIP8*-rs11064 SNP located in the 3'-UTR of *TNFAIP8* was estimated to have a MFE change of 0.6 kcal/mol with a change from A to G, and such an estimated weak change in MFE values in RNAfold models might not be seemingly consistent with the cancer risk we observed. This is likely due to limitations of the prediction tools used and the possible bias in quantitating the effect of mRNA-binding sites on secondary structures in RNAfold models (32). In a series of functional experiments, we found a decreased luciferase activity associated with the *TNFAIP8*-rs11064 A allele, a finding further validated by the *Renilla/TNFAIP8* 3'-UTR mRNA expression data in the same cell line models, also consistent with *in vivo* expression data obtained from the HapMap database. Therefore, the *TNFAIP8*-rs11064 A allele might function by affecting the affinity of *miR-22* binding to the 3'-UTR of *TNFAIP8* and thus downregulating *TNFAIP8* expression levels.

More interestingly, in the survival subset of 148 cases with cervical SCC, we found that patients with high *TNFAIP8* expression appeared to be more resistant to cisplatin and nedaplatin as well as to be more likely to have events of recurrence and death. Consistently, previous studies also showed an association of *TNFAIP8* overexpression with tumor progression and poor prognosis in cancers of the esophagus and prostate (8,42), a phenomenon that is likely due to the promotion of pre-oncogenic cells to progression to oncogenic transformation by *TNFAIP8* (43). Our findings first suggested another possible explanation for the prognostic value of *TNFAIP8* expression, which is likely under control of mechanisms other than SNPs, in cervical cancer through a

mechanism of inducing platinum resistance. Indeed, in the same subset, we did not observe any evidence for associations of *TNFAIP8* SNPs with platinum resistance and clinical outcomes, and this small sample size could lead to the lack of statistical power to indicate such an association, in addition to a short term of follow-up. On the other hand, although genetic variations may contribute to cervical cancer risk by regulating gene expression, any single SNP may be insufficient for the prediction of cancer development and prognosis (44).

Several limitations in this study need to be addressed. First, there are selection bias and information bias by the study design, which may have been minimized by frequency-matching cases and controls as well as the adjustment for potential confounding factors in final multivariate analyses. Second, because of the retrospective nature of the study design, we did not have enough information on other risk factors, especially HPV infection that may be potential confounders. This was because the hospital did not perform HPV and related subtype tests routinely for the diagnosis of all cases, let alone for the normal controls. A recent meta-analysis demonstrated that HPV16, 18 and 45 accounted for a greater or equal proportion of HPV infections in cervical cancer compared with normal cytology, but others, like high-risk HPV33, 51 and 58, were in a reverse direction (45). Therefore, the HPV infection status could be a confounder in estimating the risk associated with genetic factors.

In summary, in this case-control study of 1584 cases and 1394 controls, we found the *TNFAIP8*-rs11064 SNP to be associated with cervical cancer risk in Eastern Chinese women, and this SNP may function by affecting the affinity of *miR-22* binding to the 3'-UTR of *TNFAIP8* and regulating *TNFAIP8* expression. Furthermore, *TNFAIP8* might be a prognostic marker for cervical cancer, particularly for platinum resistance and clinical outcomes. However, well-designed larger, prospective studies with detailed information about HPV infection are warranted to validate our findings.

Supplementary material

Supplementary Tables I–VII and Figures 1 and 2 can be found at <http://carcin.oxfordjournals.org/>

Funding

China's Thousand Talents Program Recruitment at Fudan University and the Shanghai Committee of Science and Technology, China (grant no. 12DZ2260100).

Acknowledgements

We would like to thank Hong-Yu Gu, Yun-Hua Ling and Yu-Hu Xin from Fudan University Shanghai Cancer Center for their guidance on immunohistochemistry and MTT assay as well as for their technical support.

Conflict of Interest Statement: None declared.

References

- Freundt, E.C. *et al.* (2008) A different TIPE of immune homeostasis. *Cell*, **133**, 401–402.
- Lou, Y. *et al.* (2011) The TIPE (TNFAIP8) family in inflammation, immunity, and cancer. *Mol. Immunol.*, **49**, 4–7.
- Kumar, D. *et al.* (2004) Expression of SCC-S2, an antiapoptotic molecule, correlates with enhanced proliferation and tumorigenicity of MDA-MB 435 cells. *Oncogene*, **23**, 612–616.
- Cui, J. *et al.* (2011) The expression of TIPE1 in murine tissues and human cell lines. *Mol. Immunol.*, **48**, 1548–1555.
- Sun, H. *et al.* (2008) TIPE2, a negative regulator of innate and adaptive immunity that maintains immune homeostasis. *Cell*, **133**, 415–426.
- Zhang, X. *et al.* (2009) Crystal structure of TIPE2 provides insights into immune homeostasis. *Nat. Struct. Mol. Biol.*, **16**, 89–90.
- You, Z. *et al.* (2001) Nuclear factor-kappa B-inducible death effector domain-containing protein suppresses tumor necrosis factor-mediated apoptosis by inhibiting caspase-8 activity. *J. Biol. Chem.*, **276**, 26398–26404.

8. Hadisaputri, Y.E. *et al.* (2012) TNFAIP8 overexpression: clinical relevance to esophageal squamous cell carcinoma. *Ann. Surg. Oncol.*, **19** (suppl. 3), S589–S596.
9. Dong, Q.Z. *et al.* (2010) Overexpression of SCC-S2 correlates with lymph node metastasis and poor prognosis in patients with non-small-cell lung cancer. *Cancer Sci.*, **101**, 1562–1569.
10. Jemal, A. *et al.* (2011) Global cancer statistics. *CA. Cancer J. Clin.*, **61**, 69–90.
11. Walboomers, J.M. *et al.* (1999) Human papillomavirus is a necessary cause of invasive cervical cancer worldwide. *J. Pathol.*, **189**, 12–19.
12. Bedoya, A.M. *et al.* (2012) Location and density of immune cells in precursor lesions and cervical cancer. *Cancer Microenviron.*, doi:10.1007/s12307-012-0097-8.
13. Bartel, D.P. (2004) MicroRNAs: genomics, biogenesis, mechanism, and function. *Cell*, **116**, 281–297.
14. Lewis, B.P. *et al.* (2005) Conserved seed pairing, often flanked by adenosines, indicates that thousands of human genes are microRNA targets. *Cell*, **120**, 15–20.
15. Zamore, P.D. *et al.* (2005) Ribo-gnome: the big world of small RNAs. *Science*, **309**, 1519–1524.
16. Liu, Z. *et al.* (2011) A functional variant at the miR-184 binding site in TNFAIP2 and risk of squamous cell carcinoma of the head and neck. *Carcinogenesis*, **32**, 1668–1674.
17. Chen, A.X. *et al.* (2011) Germline genetic variants disturbing the Let-7/LIN28 double-negative feedback loop alter breast cancer susceptibility. *PLoS Genet.*, **7**, e1002259.
18. Ratner, E.S. *et al.* (2012) A KRAS variant is a biomarker of poor outcome, platinum chemotherapy resistance and a potential target for therapy in ovarian cancer. *Oncogene*, **31**, 4559–4566.
19. Shi, T.Y. *et al.* (2013) Polymorphisms of the interleukin 6 gene contribute to cervical cancer susceptibility in Eastern Chinese women. *Hum. Genet.*, **132**, 301–312.
20. WHO. (2010) World Health Organization. International histological classification of tumours. Available at who.int/classifications/icd/en/ (last accessed 6 July 2012).
21. Cheng, X. *et al.* (2008) Concurrent chemotherapy and adjuvant extended field irradiation after radical surgery for cervical cancer patients with lymph node metastases. *Int. J. Gynecol. Cancer*, **18**, 779–784.
22. He, J. *et al.* (2012) Polymorphisms in the XPG gene and risk of gastric cancer in Chinese populations. *Hum. Genet.*, **131**, 1235–1244.
23. An, Y. *et al.* (2010) A QuikChange-like method to realize efficient blunt-ended DNA directional cloning and site-directed mutagenesis simultaneously. *Biochem. Biophys. Res. Commun.*, **397**, 136–139.
24. Livak, K.J. *et al.* (2001) Analysis of relative gene expression data using real-time quantitative PCR and the 2⁻(delta delta C(T)) method. *Methods*, **25**, 402–408.
25. Holm, K. *et al.* (2010) SNPexp - A web tool for calculating and visualizing correlation between HapMap genotypes and gene expression levels. *BMC Bioinformatics*, **11**, 600.
26. Shi, T.Y. *et al.* (2012) Association between XPF polymorphisms and cancer risk: a meta-analysis. *PLoS ONE*, **7**, e38606.
27. Cheng, X. *et al.* (2011) Recurrence patterns and prognosis of endometrial stromal sarcoma and the potential of tyrosine kinase-inhibiting therapy. *Gynecol. Oncol.*, **121**, 323–327.
28. Yamaue, H. *et al.* (1991) Chemosensitivity testing with highly purified fresh human tumour cells with the MTT colorimetric assay. *Eur. J. Cancer*, **27**, 1258–1263.
29. Shi, T.Y. *et al.* (2012) RAD52 variants predict platinum resistance and prognosis of cervical cancer. *PLoS ONE*, **7**, e50461.
30. WHO. (2009) World Health Organization. Global database on body mass index. Available at apps.who.int/bmi/index.jsp (last accessed 6 July 2012).
31. Wacholder, S. *et al.* (2004) Assessing the probability that a positive report is false: an approach for molecular epidemiology studies. *J. Natl. Cancer Inst.*, **96**, 434–442.
32. Kertesz, M. *et al.* (2007) The role of site accessibility in microRNA target recognition. *Nat. Genet.*, **39**, 1278–1284.
33. Patel, S. *et al.* (1997) Identification of seven differentially displayed transcripts in human primary and matched metastatic head and neck squamous cell carcinoma cell lines: implications in metastasis and/or radiation response. *Oral Oncol.*, **33**, 197–203.
34. Kumar, D. *et al.* (2000) Identification of a novel tumor necrosis factor-alpha-inducible gene, SCC-S2, containing the consensus sequence of a death effector domain of fas-associated death domain-like interleukin-1beta-converting enzyme-inhibitory protein. *J. Biol. Chem.*, **275**, 2973–2978.
35. Woodward, M.J. *et al.* (2010) Tnfaip8 is an essential gene for the regulation of glucocorticoid-mediated apoptosis of thymocytes. *Cell Death Differ.*, **17**, 316–323.
36. Zhang, Y. *et al.* (2012) Tumor necrosis factor- α induced protein 8 polymorphism and risk of non-Hodgkin's lymphoma in a Chinese population: a case-control study. *PLoS ONE*, **7**, e37846.
37. Lui, W.O. *et al.* (2007) Patterns of known and novel small RNAs in human cervical cancer. *Cancer Res.*, **67**, 6031–6043.
38. Hu, X. *et al.* (2010) A microRNA expression signature for cervical cancer prognosis. *Cancer Res.*, **70**, 1441–1448.
39. Saunders, M.A. *et al.* (2007) Human polymorphism at microRNAs and microRNA target sites. *Proc. Natl. Acad. Sci. U.S.A.*, **104**, 3300–3305.
40. Zhou, X. *et al.* (2010) Polymorphisms involved in the miR-218-LAMB3 pathway and susceptibility of cervical cancer, a case-control study in Chinese women. *Gynecol. Oncol.*, **117**, 287–290.
41. Reshmi, G. *et al.* (2011) C-T variant in a miRNA target site of BCL2 is associated with increased risk of human papilloma virus related cervical cancer—an in silico approach. *Genomics*, **98**, 189–193.
42. Romanuik, T.L. *et al.* (2009) Novel biomarkers for prostate cancer including noncoding transcripts. *Am. J. Pathol.*, **175**, 2264–2276.
43. Laliberté, B. *et al.* (2010) TNFAIP8: a new effector for Galpha(i) coupling to reduce cell death and induce cell transformation. *J. Cell. Physiol.*, **225**, 865–874.
44. Galvan, A. *et al.* (2010) Beyond genome-wide association studies: genetic heterogeneity and individual predisposition to cancer. *Trends Genet.*, **26**, 132–141.
45. Guan, P. *et al.* (2012) Human papillomavirus types in 115,789 HPV-positive women: a meta-analysis from cervical infection to cancer. *Int. J. Cancer*, **131**, 2349–2359.

Received August 13, 2012; revised November 27, 2012; accepted December 29, 2012